

# Kinetics and Mechanism of Base Hydrolysis in Cobalt(III) Complexes – The Case of a Complex $\text{CoLCl}^{2+}$ where L has the Novel Topology of a Square-Pyramidal $\text{NN}_4$ Coordination Cap

Tilo Poth,<sup>[a]</sup> Helmut Paulus,<sup>[a]†</sup> Horst Elias,<sup>\*[a]</sup> Rudi van Eldik,<sup>[b]</sup> and Andreas Grohmann<sup>\*[b]</sup>

**Keywords:** Cobalt(III) complexes / Tetrapodal pentadentate ligand / Hydrolysis / Kinetics / Mechanism

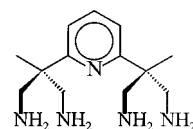
Multi-wavelength stopped-flow spectrophotometry was used to study the kinetics of base hydrolysis of the octahedral cobalt(III) complex  $\text{CoLCl}^{2+}$  (**2**), in which the tetrapodal pentadentate ligand L has an  $\text{NN}_4$  donor set and forms a square-pyramidal coordination cap [L = 2,6-bis(1',3'-diamino-2'-methylprop-2'-yl)pyridine, **1**]. The kinetic investigation, carried out at different temperatures, pressures and ionic strengths *I*, led to second-order kinetics, rate =  $k_{\text{OH}}[2][\text{OH}^-]$ , with  $k_{\text{OH}} = 0.139 \pm 0.001 \text{ M}^{-1}\text{s}^{-1}$  (*I* = 0.1 M) and  $k_{\text{OH}} = 0.0570 \pm 0.0004 \text{ M}^{-1}\text{s}^{-1}$  (*I* = 1.0 M) at 298 K. The temperature and pressure dependence of  $k_{\text{OH}}$  resulted in  $\Delta H^\ddagger = 119 \pm 3 \text{ kJmol}^{-1}$  (*I* = 0.1 M) and  $\Delta H^\ddagger = 123 \pm 3 \text{ kJmol}^{-1}$  (*I* = 1.0 M),  $\Delta S^\ddagger = +130 \pm 13 \text{ Jmol}^{-1}\text{K}^{-1}$  (*I* = 0.1 M) and  $\Delta S^\ddagger = +151 \pm 15 \text{ Jmol}^{-1}\text{K}^{-1}$  (*I* = 1.0 M) and  $\Delta V^\ddagger = +27.6 \pm 0.6 \text{ cm}^3\text{mol}^{-1}$  (*I* = 1.0 M). The kinetic results support the operation of the conjugate base mechanism,  $\text{D}_{\text{cb}}$ , with intermediate deprotonation occurring *cis* to the leaving chloride ion. The observed

inertness of complex **2** towards base hydrolysis is discussed on the basis of the special structural features of the ligand L. The  $\text{pK}_{\text{a}}$  of the coordinated water in the aqua species  $\text{CoL}(\text{H}_2\text{O})^{3+}$  (**3**) was determined to be  $\text{pK}_{\text{a}} = 6.0 \pm 0.1$  at *I* = 0.1 M. The X-ray crystal structure analysis of the hydroxo complex  $[\text{CoL}(\text{OH})](\text{ClO}_4)_2$  (**4**) shows a mononuclear terminal (hydroxo)Co<sup>III</sup> complex, in which the ligand provides a regular square-pyramidal  $\text{NN}_4$  donor cap for the octahedrally six-coordinate Co<sup>III</sup> ion [**4**, monoclinic, space group *C2/m*, *a* = 16.841(6) Å, *b* = 8.541(3) Å, *c* = 15.112(5) Å,  $\beta = 109.13(1)^\circ$ , *Z* = 4]. Coordination of L is accompanied by the formation of 6 six-membered chelate rings, all of which adopt a boat conformation. In the crystal lattice, pairs of cations are associated via four (hydroxo)O⋯H–N(primary amine) hydrogen bonds and related through an inversion center. Full spectroscopic data for **4** (<sup>1</sup>H-, <sup>13</sup>C-NMR, IR, MS) are presented.

## Introduction

Tetrapodal pentadentate ligands designed to provide a square-pyramidal coordination cap for octahedrally coordinating transition metal ions were until recently unknown.<sup>[1–3]</sup> This coordination mode requires a ligand to have an apical donor atom with a lone pair oriented towards the center of the octahedron, while four donor groups are juxtaposed to occupy the equatorial positions. The interest in ligands of this type arises from their potential stabilization of free coordination sites in otherwise octahedrally coordinated complexes. Suitable derivatization of the equatorial positions may then provide an environment for a monodentate substrate or reagent (such as metal-coordinated hydroxide) in which it shows modulated reactivity.<sup>[4]</sup>

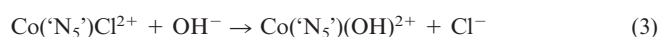
The coordination behavior of the prototypical  $\text{NN}_4$  coordination cap **1** ( $\equiv$  L) towards nickel(II) and cobalt(III) has been the subject of recent work.<sup>[2,5,6]</sup> The ligand acts as a podand in all cases (including a  $\text{Co}^{\text{III}}\text{--CH}_3$  complex), and



**1** ( $\equiv$  L)

a polynuclear coordination mode has not been observed. Given the similarity of pyridine and ammine ligands with respect to their position in the spectrochemical series, **1** may be considered a highly symmetrical chelating analogue of the classical pentaammine donor set, and complexes of **1** are expected to show similar reactivity, e.g. with respect to ligand exchange. In order to substantiate this assumption and obtain mechanistic data relevant to future use of the ligand as a mononucleating head group in functional metal complexes, we chose to study the kinetics of a classical exchange reaction of cobalt(III), viz. the base-assisted hydrolysis of  $\text{CoLCl}^{2+}$  (**2**).

Base-assisted hydrolysis of the octahedral Werner-type complex  $\text{Co}(\text{NH}_3)_5\text{Cl}^{2+}$  according to Equation 1, following the simple rate law of Equation 2, has initiated an impressive number of kinetic studies on reactions of Equation 3.<sup>[7]</sup>



<sup>[†]</sup> Technische Universität Darmstadt, Fachbereich Materialwissenschaft

<sup>[a]</sup> Institut für Anorganische Chemie, Technische Universität Darmstadt, Petersenstraße 18, D-64287 Darmstadt, Germany  
E-mail: elias@hrz1.hrztu-darmstadt.de

<sup>[b]</sup> Institut für Anorganische Chemie, Universität Erlangen-Nürnberg, Egerlandstraße 1, D-91058 Erlangen, Germany  
E-mail: grohmann@anorganik.chemie.uni-erlangen.de

These reactions are now commonly agreed to proceed by the so-called "conjugate base mechanism",  $D_{cb}$  (formerly  $S_N1CB$ ), which involves the intermediate formation of a substitutionally labile amide complex.<sup>[8,9]</sup> The symbol ' $N_5$ ' in Equation 3 stands for a set of five N donor atoms in the form of either five monodentate ligands or combinations of monodentate and chelate ligands, such as  $(N + N_2 + N_2)$ ,  $(N_2 + N_3)$ ,  $(N + N_4)$ , and  $(N_5)$ .

Such variations in the ' $N_5$ ' set of ligands were made in order to allow meaningful conclusions concerning, for example, the question of deprotonation and amide bond formation *cis* or *trans* to the leaving group. An interesting outcome of these studies was that the nature of the ligands making up ' $N_5$ ' has a pronounced effect on the magnitude of the second-order rate constant  $k_{OH}$ , which reflects the kinetic significance of the structural features in the ' $N_5$ ' coordination sphere.

The  $NN_4$  topology of L in the octahedral chlorocobalt complex  $[CoLCl]Cl(ClO_4) \cdot H_2O$ <sup>[2]</sup> represents a novel type of ' $N_5$ ' unit. In view of the individual steps associated with the  $D_{cb}$  mechanism, the situation in this complex is remarkable for several reasons. Firstly, the nitrogen atom *trans* to the leaving group is tertiary, hence cannot be deprotonated. Since pyridine donors coordinated *cis* to the leaving group were found to increase the rate of base hydrolysis markedly,<sup>[10]</sup> species in which pyridine is coordinated *trans* to the leaving group have long been called for for the purpose of comparison.<sup>[11,12]</sup> Secondly, the ligand L enforces a rigid square-pyramidal coordination cap containing four equivalent  $Co-NH_2R$  bonds, which raises the question whether the internal steric strain associated with the deprotonation of one of the  $NH_2$  groups is possibly too high to allow intermediate amide bond formation at all.

The present contribution provides the kinetic data obtained for the reaction according to Equation 3 at different temperatures, pressures and ionic strengths, as well as spectroscopic and X-ray structural data for the hydroxo complex  $[CoL(OH)](ClO_4)_2$  (**4**). The  $pK_a$  value of the aqua complex  $CoL(H_2O)^{3+}$  (**3**) is also reported.

## Results and Discussion

### Properties of the Complexes

Table 1 summarizes the UV/Vis absorption data of the cations **2**, **4**, and **3**. The spectra show two absorption maxima, which can be assigned to the transitions  $^1T_{1g} \leftarrow ^1A_{1g}$  and  $^1T_{2g} \leftarrow ^1A_{1g}$ , commonly observed in  $Co^{III}$  complexes of this type. The variation of the sixth ligand ( $Cl^- \rightarrow OH^- \rightarrow H_2O$ ) causes a blue shift of both maxima ( $\lambda_{max} = 356 \rightarrow 343 \rightarrow 335$  nm and  $\lambda_{max} = 512 \rightarrow 480 \rightarrow 480$  nm), which is in accord with the position of the ligands in the spectrochemical series.

Table 1. Visible absorption  $\{\lambda_{max}$  [nm] ( $\epsilon_{max}$  [ $M^{-1}cm^{-1}$ ]) of the complex cations in aqueous solution at 293 K

$CoL(Cl)^{2+}$ ( <b>2</b> )	356(101)	512(67)
$CoL(OH)^{2+}$ ( <b>4</b> )	343(128)	480(95)
$CoL(H_2O)^{3+}$ ( <b>3</b> )	335(100)	480(56)

Figure 1 shows the spectral changes following the step-wise deprotonation of the species **3** according to Equation 4 and, as an example, the plot of  $A_{483}$  vs pH. Multi-wavelength fitting of the ( $A$ ,  $[H^+]$ ) data (350–600 nm) with Equation 5 leads to  $pK_a = 6.0 \pm 0.1$ . The  $pK_a$  found for complex **3** is very similar to the  $pK_a$  reported for other (amine)(monoaqua)cobalt(III) complexes.<sup>[13]</sup> From its magnitude it follows that even at pH = 5–6 appreciable amounts of the hydroxo species **4** are present.



$$A = \{A_{H_2O} + A_{OH}(K_a)^{-1}[H^+]\} / \{1 + (K_a)^{-1}[H^+]\} \quad (5)$$

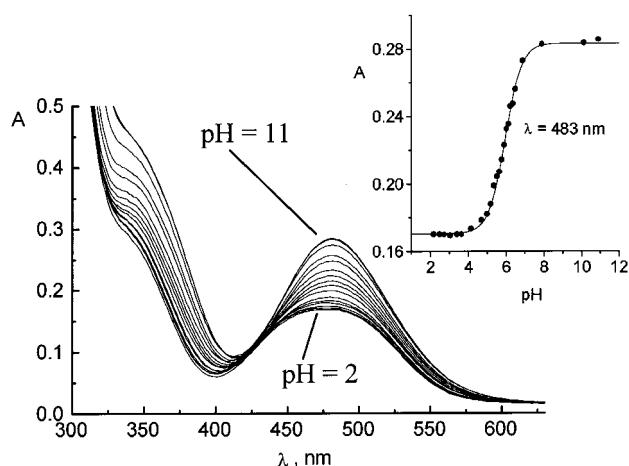


Figure 1. Spectral changes associated with the titration of complex **3** ( $3 \cdot 10^{-3}$  M) with 0.1 M NaOH at 298 K and  $I = 0.1$  M ( $NaNO_3$ ); insert: plot of  $A_{483}$  vs. pH and fit (solid line) with Equation 5

The  $^1H$ - and  $^{13}C$ -NMR spectra of **4** (r.t.; amount of sample: 20 mg; solvent: anhydrous  $[D_6]DMSO$ ; amount of solvent: 0.6 mL) largely resemble those of the parent chloro complex  $[CoLCl]Cl(ClO_4) \cdot H_2O$  in terms of chemical shift and signal multiplicity.<sup>[2]</sup> A few features deserve special mention. In the  $^1H$ -NMR spectrum of **4**, the resonances of the diastereotopic amine protons ( $\delta = 4.52$  and 4.70) are shielded by ca. 0.8 ppm and 1.2 ppm, respectively, relative to the corresponding resonances in  $[CoLCl]Cl(ClO_4) \cdot H_2O$  ( $\delta = 5.29$  and 5.85). There is a broad singlet at high field, viz.  $-2.60$  (sweep width  $-20$  to  $+30$  ppm;  $W_{1/2} = 7.1$  Hz), which we assign to the proton of the hydroxo ligand. The observed high-field shift is presumably a consequence of the OH proton being solitary, i.e. not involved in hydrogen bonding under the given conditions. Hydrogen bonding, if present, as well as the electronegative nature of the heteroatom carrying this proton, would lead one to expect a significant *downfield* shift of its resonance. The signal disappears owing to exchange when water is allowed to diffuse into the sample. We are not aware of reliable previous NMR data of structurally characterised  $Co^{III}$  complexes containing a terminal hydroxo ligand. In a structurally characterised monomeric terminal hydroxo complex of zinc, the  $Zn-OH$  resonance is observed at similarly high field ( $\delta = -0.06$ ; solvent:  $[D_6]benzene$ ).<sup>[14]</sup> In the  $^{13}C$ -NMR spectrum of **4**, the resonance assigned to the methylene carbon atoms

shows fine structure. An asymmetric three-line signal is observed ( $J = 7.8$  Hz), of which the line towards low field is not well resolved but is visible as a shoulder. We attribute this splitting to partially resolved coupling with the  $^{14}\text{N}$  nucleus ( $I = 1$ ), which is usually only observable in highly symmetric species such as tetraalkylammonium ions, in which the electric field gradient at  $^{14}\text{N}$  is zero or sufficiently small.<sup>[15]</sup>

In the IR spectrum of **4**, there is a sharp  $\nu(\text{OH})$  str band of medium intensity at  $3578\text{ cm}^{-1}$ . A band below  $1200$  to  $700\text{ cm}^{-1}$ , characteristic of a hydroxo complex and due to the  $\text{M}-\text{O}-\text{H}$  bending vibration,<sup>[16]</sup> cannot be assigned with certainty as this region is obscured by the very broad absorption of the  $\text{ClO}_4^-$  counterions.

### Structure of the Complex $[\text{CoL}(\text{OH})](\text{ClO}_4)_2$ (**4**)

The X-ray structure analysis unequivocally confirms the presence of a mononuclear terminal (hydroxo) $\text{Co}^{\text{III}}$  complex, making **4** one of the very few examples of such complexes that have been structurally characterised.<sup>[17]</sup> The molecular structure of the cation, which has crystallographically imposed mirror symmetry, is shown in Figure 2. Selected bond lengths and angles are given in Table 2. The mirror plane contains the pyridine ring, the quaternary and methyl carbon atoms of the pentaamine ligand backbone, one of the protons on each exocyclic methyl group, the cobalt atom, and the oxygen and hydrogen atoms of the hydroxo ligand. All hydrogen atoms have been located in the difference Fourier map. Specifically, the location of electron density corresponding to *one* proton bound to the hydroxo oxygen atom is clearly discernible at a reasonable distance and angle relative to that atom [ $d(\text{O}-\text{H}) = 0.863(2)\text{ \AA}$ ,  $\angle\text{Co}-\text{O}-\text{H} = 109.9(2)^\circ$ ]. There is no residual electron density in the vicinity of the hydroxo ligand.

The pentaamine ligand coordinates to cobalt(III) in pyramidal fashion, with the pyridine nitrogen atom occupying an axial position of the overall coordination octahedron, while the four equivalent amino nitrogen atoms take the equatorial positions. This mode of coordination leads to the formation of 6 six-membered chelate rings, all of which adopt a boat conformation. The hydroxo ligand occupies the remaining axial position. The coordination octahedron is close to regular, with angles  $\text{N}_{\text{ax}}-\text{Co}-\text{N}_{\text{eq}}$  and  $\text{N}_{\text{eq}}-\text{Co}-\text{N}_{\text{eq}}$  ranging from  $84.91(10)^\circ$  to  $93.16(7)^\circ$ . The arrangement of atoms along the principal axis of the octahedron ( $\text{N11}$ ,  $\text{Co1}$ ,  $\text{O1}$ ) is linear [ $179.77(8)^\circ$ ], and the angles between diametrically disposed pairs of  $\text{NH}_2$  substituents ( $\text{N12}$ ,  $\text{N13}'$ ;  $\text{N12}'$ ,  $\text{N13}$ ) at  $\text{Co}$  are close to  $180^\circ$  [ $175.94(7)^\circ$ ]. The cobalt atom is displaced from the plane defined by the four equatorial amino nitrogen atoms towards the pyridine N atom by only  $0.044(1)\text{ \AA}$ . The pyridine ring is a regular hexagon. Thus, the tetrapodal pentadentate amine ligand provides a square-pyramidal coordination cap for the metal center in the same way as in a related chloro<sup>[2]</sup> and methyl complex.<sup>[6]</sup> The cobalt–pyridine bond length in **4** [ $1.934(2)\text{ \AA}$ ] is the same within experimental error as that in the

chloro complex  $[\text{CoLCl}]\text{Cl}(\text{ClO}_4)_4 \cdot \text{H}_2\text{O}$  [ $1.928(3)\text{ \AA}$ ],<sup>[2]</sup> as opposed to a value of  $2.018(2)\text{ \AA}$  for the corresponding bond in the methyl complex  $[\text{CoL}(\text{CH}_3)]\text{S}_2\text{O}_6$ .<sup>[6]</sup> This reflects *trans* influences of comparable magnitude for  $\text{OH}^-$  and  $\text{Cl}^-$ , as opposed to the significantly larger *trans* influence exerted by the  $\text{CH}_3^-$  ligand.<sup>[18]</sup> The  $\text{Co1}-\text{O1}$  distance in **4** [ $1.897(2)\text{ \AA}$ ] is comparable to the value obtained for another terminal  $\text{Co}^{\text{III}}-\text{OH}$  complex [ $1.894(10)\text{ \AA}$ ],<sup>[17b]</sup> while the value determined for a third complex [ $2.190(3)\text{ \AA}$ ] is so large as to have been considered at odds with the formulation as a hydroxo species.<sup>[17a]</sup>

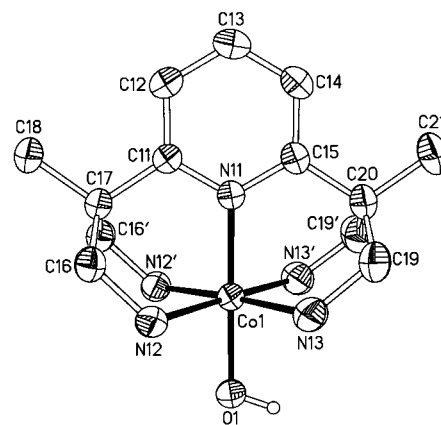


Figure 2. Molecular structure of **4** with thermal ellipsoids drawn at the 50% probability level; the position of the hydroxo hydrogen atom H1 is indicated by a sphere of arbitrary diameter; all other hydrogen atoms have been omitted for clarity

Table 2. Selected distances and angles for  $[\text{CoL}(\text{OH})](\text{ClO}_4)_2$  (**4**)

Atoms	Distance [ $\text{\AA}$ ]	Atoms	Distance [ $\text{\AA}$ ]
$\text{Co1}-\text{N11}$	1.934(2)	$\text{Co1}-\text{N13}$	1.958(2)
$\text{Co1}-\text{N12}$	1.963(2)	$\text{Co1}-\text{O1}$	1.897(2)
$\text{O1}-\text{H1}$	0.863(2)		
Atoms	Angle [ $^\circ$ ]	Atoms	Angle [ $^\circ$ ]
$\text{N11}-\text{Co1}-\text{O1}$	179.77(8)	$\text{C12}-\text{C11}-\text{C17}$	122.8(3)
$\text{Co1}-\text{O1}-\text{H1}$	109.9(2)	$\text{C14}-\text{C15}-\text{C20}$	122.2(3)
$\text{N11}-\text{Co1}-\text{N12}$	93.16(7)	$\text{C11}-\text{C17}-\text{C18}$	110.9(2)
$\text{N11}-\text{Co1}-\text{N13}$	89.53(7)	$\text{C15}-\text{C20}-\text{C21}$	112.3(3)
$\text{O1}-\text{Co1}-\text{N12}$	87.01(7)	$\text{C11}-\text{C17}-\text{C16}$	109.9(1)
$\text{O1}-\text{Co1}-\text{N13}$	90.31(7)	$\text{C15}-\text{C20}-\text{C19}$	109.8(2)
$\text{N12}-\text{Co1}-\text{N12}'$	84.92(10)	$\text{C16}-\text{C17}-\text{C18}$	107.0(1)
$\text{N12}-\text{Co1}-\text{N13}$	91.91(9)	$\text{C19}-\text{C20}-\text{C21}$	107.1(2)
$\text{N13}-\text{Co1}-\text{N13}'$	91.15(12)	$\text{C16}-\text{C17}-\text{C16}'$	112.0(2)
$\text{N12}-\text{Co1}-\text{N13}'$	175.94(7)	$\text{C19}-\text{C20}-\text{C19}'$	110.8(3)
$\text{C11}-\text{N11}-\text{Co1}$	120.1(2)	$\text{C17}-\text{C16}-\text{N12}$	112.9(2)
$\text{C15}-\text{N11}-\text{Co1}$	119.8(2)	$\text{C20}-\text{C19}-\text{N13}$	113.7(2)
$\text{N11}-\text{C11}-\text{C17}$	116.7(2)	$\text{C16}-\text{N12}-\text{Co1}$	117.5(1)
$\text{N11}-\text{C15}-\text{C20}$	117.5(2)	$\text{C19}-\text{N13}-\text{Co1}$	118.7(2)

In the crystal lattice, pairs of cations are associated via (hydroxo) $\text{O}\cdots\text{H}-\text{N}(\text{primary amine})$  hydrogen bonds and related through an inversion center as follows: Both lone pairs on the hydroxo ligand of cation 1(2) receive hydrogen bonds from one proton each on two adjacent amino groups in cation 2(1). The distance  $\text{O1}\cdots\text{N12}$  is  $2.874(2)\text{ \AA}$ , and the angle at H12A is  $151.8(1)^\circ$  (sum of the van der Waals radii of O and N:  $3.07\text{ \AA}$ <sup>[19]</sup>). The hydroxo protons of cation 1 and 2 point away from each other and do not participate

in hydrogen bonding. The crystallographic inversion center is located at the midpoint of the vector connecting the hydroxo oxygen atoms of cation 1 and 2. The other non-bonded distances in the crystal packing fall outside the range where significant hydrogen bonding may be inferred. The two perchlorate counterions show rotational disorder which has been resolved, but otherwise have normal structural parameters. The residual electron density in the overall structure is located at  $\text{ClO}_4^-$ .

### Kinetics of Base Hydrolysis

As shown in Figure 3 for  $\text{pH} \approx 12$ , base hydrolysis of complex **2**, as obtained by dissolving  $[\text{CoLCl}]\text{Cl}(\text{ClO}_4) \cdot \text{H}_2\text{O}$  in water, is associated with substantial spectral changes and occurs with a half-life of several minutes ( $T = 298 \text{ K}$ ). The  $(A, t)$  data can be fitted very satisfactorily to one exponential (Equation 6) for the whole wavelength range. Experiments carried out in the presence of a thirtyfold excess of  $\text{NaCl}$  guaranteed that non-coordinated chloride ions, as introduced with the complex  $[\text{CoLCl}]\text{Cl}(\text{ClO}_4) \cdot \text{H}_2\text{O}$ , have no effect on the magnitude of the experimental rate constant  $k_{\text{obsd}}$ .

$$A = (A_0 - A_\infty)[\exp(-k_{\text{obsd}}t)] + A_\infty \quad (6)$$

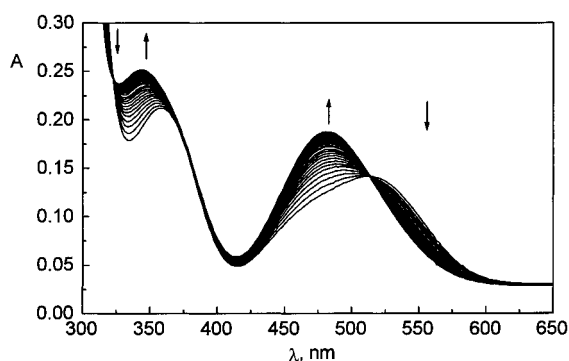


Figure 3. Spectral changes associated with the base hydrolysis of complex **2** ( $2.2 \cdot 10^{-3} \text{ M}$ ) at  $\text{pH} \approx 12$  and  $293 \text{ K}$  (the spectra, taken at time intervals of  $19.8 \text{ s}$ , cover a reaction time of  $990 \text{ s}$ )

Figure 4 shows that the dependence of  $k_{\text{obsd}}$  on  $[\text{OH}^-]$  is linear, which leads to the rate law of Equation 7 and second-order rate constant  $k_{\text{OH}}$ .

$$\text{rate} = -d[\text{CoLCl}^{2+}]/dt = d[\text{CoL}(\text{OH})^{2+}]/dt = k_{\text{OH}}[\text{CoLCl}^{2+}][\text{OH}^-] \quad (7)$$

In addition, Figure 4 documents that the rate of base hydrolysis increases with decreasing ionic strength, as expected for the reaction between species of opposite charge.<sup>[20]</sup> The observed ratio for  $k_{\text{OH}} (I = 0.1 \text{ M})/k_{\text{OH}} (I = 1.0 \text{ M}) = 2.4$  is in accord with the averaged value  $k_{\text{OH}} (I =$

$0.1 \text{ M})/k_{\text{OH}} (I = 1.0 \text{ M}) = 2.2$ , as reported earlier for a number of  $\text{Co}'\text{N}_5'\text{X}^{2+}$  complexes.<sup>[11]</sup>

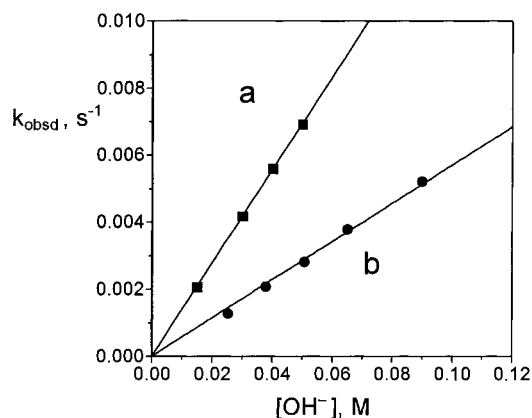
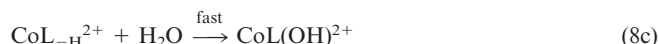
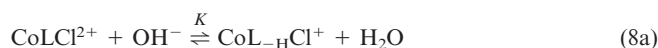


Figure 4. Plot of the experimental rate constant  $k_{\text{obsd}}$  vs.  $[\text{OH}^-]$  for base hydrolysis of complex **2** ( $2.2 \cdot 10^{-3} \text{ M}$ ) according to Equation 7 at  $I = 0.1 \text{ M NaClO}_4$  (a) and  $I = 1.0 \text{ M NaNO}_3$  (b), ( $T = 298 \text{ K}$ )

Least-squares fitting of the data shown in Figure 3 leads to  $k_{\text{OH}} = 0.139 \text{ M}^{-1}\text{s}^{-1}$  ( $I = 0.1 \text{ M}$ ) and  $k_{\text{OH}} = 0.0570 \text{ M}^{-1}\text{s}^{-1}$  ( $I = 1.0 \text{ M}$ ). These rate constants are amongst the lowest ever reported for base hydrolysis reactions of Equation 3.<sup>[21]</sup>

The  $\text{D}_{\text{cb}}$  mechanism is based on the reaction sequence of Equations 8a–8c, with Equation 8a being a fast deprotonation/protonation equilibrium and Equation 8b being the rate-determining step which, as pointed out, is very slow in the present system (the symbol  $\text{L}_{-\text{H}}$  stands for the ligand  $\text{L}$ , mono-deprotonated at one of the four primary amino groups).



Assuming the equilibrium according to Equation 8a to be established and  $[\text{complex}]_0 \ll [\text{OH}^-]$ , one can derive the rate law of Equation 9 which suggests that the dependence  $k_{\text{obsd}} = f([\text{OH}^-])$  should come to saturation for  $K[\text{OH}^-] \gg 1$ .

$$d[\text{CoL}(\text{OH})^{2+}]/dt = \{k \cdot K[\text{OH}^-]/(1 + K[\text{OH}^-])\} \cdot [\text{CoLCl}^{2+}] = k_{\text{obsd}}[\text{CoLCl}^{2+}] \quad (9)$$

As shown in Figure 4,  $k_{\text{obsd}}$  increases linearly with  $[\text{OH}^-]$  up to  $[\text{OH}^-] = 0.09 \text{ M}$ . This means that the estimate  $K[\text{OH}^-] \ll 1$  can be made, for which condition the rate law of Equation 9 takes the simple form of Equation 10 which corresponds to the experimentally found rate law of Equation 2 with  $k_{\text{OH}} \equiv k \cdot K$ .

$$d[\text{CoL}(\text{OH})^{2+}]/dt = k \cdot K[\text{OH}^-] \cdot [\text{CoLCl}^{2+}] \quad (10)$$

It is noteworthy that a linear dependence of  $k_{\text{OH}}$  on  $[\text{OH}^-]$  is generally observed for the base hydrolysis of cobalt(III) complexes.<sup>[9]</sup>



Table 3. Kinetic parameters for the base hydrolysis of some cobalt(III) complexes of the type  $\text{Co}(\text{N}_5)\text{Cl}^{2+}$  according to Equation 3

Complex	$I$ [M]	$k_{\text{OH}}^{298}$ [ $\text{M}^{-1}\text{s}^{-1}$ ]	$\Delta H^\ddagger$ [ $\text{kJ mol}^{-1}$ ] <sup>[a]</sup>	$\Delta S^\ddagger$ [ $\text{Jmol}^{-1}\text{K}^{-1}$ ] <sup>[a]</sup>	$\Delta V^\ddagger_{\text{exptl}}$ [ $\text{cm}^3 \text{mol}^{-1}$ ] <sup>[a]</sup>	Ref.
$\text{Co}(\text{NH}_3)_5\text{Cl}^{2+}$	0.1	0.86	118	+155	+33.8 ± 1.0	[28][33]
$\text{Co}(\text{L})\text{Cl}^{2+}$ ( <b>2</b> )	0.1	0.1389 ± 0.0009	119 ± 3	+130 ± 13	—	this work
	1.0	0.0570 ± 0.0004	123 ± 3	+151 ± 15	+27.6 ± 0.6	this work
<i>cis</i> - $\text{Co}(\text{en})_2(\text{NH}_3)\text{Cl}^{2+[\text{b}]}$	—	54.0	—	—	+31.8 ± 0.6	[24][33]
<i>t</i> - $\text{Co}(\text{tren})(\text{NH}_3)\text{Cl}^{2+[\text{c}]}$	1.0	0.02 ± 0.003	—	—	—	[34]
<i>p</i> - $\text{Co}(\text{tren})(\text{NH}_3)\text{Cl}^{2+[\text{c}]}$	1.0	3.8 ± 0.2	—	—	—	[34]
<i>a</i> - $\text{Co}(\text{tmd})(\text{dien})\text{Cl}^{2+[\text{d}]}$	0.1	(5.02 ± 0.14) × 10 <sup>5</sup>	81 ± 3	+135 ± 4	—	[25]
<i>d</i> - $\text{Co}(\text{tmd})(\text{dien})\text{Cl}^{2+[\text{d}]}$	0.1	138	89 ± 2	+94 ± 3	—	[25]
<i>h</i> - $\text{Co}(\text{tmd})(\text{dien})\text{Cl}^{2+[\text{d}]}$	0.1	10.6	120 ± 3	+179 ± 6	—	[25]
$\text{Co}(\text{en})_2(\text{py})\text{Cl}^{2+}$	0.1	332 ± 4	83.6 ± 0.8	+84 ± 2	—	[10]
$\text{Co}(\text{tacn})(\text{amp})\text{Cl}^{2+[\text{e}]}$	0.1	154 ± 5	—	—	—	[11]
	1.0	66.7 ± 2.3	83.3 ± 1.2	+69 ± 4	—	[11]

<sup>[a]</sup>  $\Delta H^\ddagger$  and  $\Delta S^\ddagger$  were obtained from the temperature dependence of  $k_{\text{OH}}$  at five temperatures in the range  $T = 285\text{--}318$  K.  $\Delta V^\ddagger_{\text{exptl}}$  was obtained from the pressure dependence of the first-order rate constant  $k_{\text{obsd}}$  in the range 10–150 MPa at 308 K. — <sup>[b]</sup> en = 1,2-Diaminoethane ( $\text{NH}_2[\text{CH}_2]_2\text{NH}_2$ ). — <sup>[c]</sup> tren = Tris(2-aminoethyl)amine [ $\text{N}(\text{CH}_2\text{CH}_2\text{NH}_2)_3$ ]; *t* isomer: tertiary nitrogen atom *trans* to coordinated chloride, *p* isomer: tertiary nitrogen atom *cis* to coordinated chloride. — <sup>[d]</sup> tmd = 1,3-Diaminopropane ( $\text{NH}_2[\text{CH}_2]_3\text{NH}_2$ ); dien = 3-azapentane-1,5-diamine ( $\text{NH}_2[\text{CH}_2]_2\text{NH}[\text{CH}_2]_2\text{NH}_2$ ); *a* isomer: “flat” nitrogen atom of dien *cis* to coordinated chloride; *d* isomer: “bent” nitrogen atom of dien *cis* to coordinated chloride; *h* isomer: “bent” nitrogen atom of dien *trans* to coordinated chloride. — <sup>[e]</sup> tacn = 1,4,7-Triazacyclononane; amp = 2-aminomethylpyridine.

It has been shown that anion competition experiments<sup>[22,23]</sup> and the determination of reaction volume profiles<sup>[24]</sup> can provide experimental evidence for the validity of the commonly accepted  $\text{D}_{\text{cb}}$  mechanism. In order to substantiate the operation of the  $\text{D}_{\text{cb}}$  mechanism for the base hydrolysis of **2**, experiments at different temperatures (see Table 4) and pressures (see Figure 5) were carried out. The resulting activation parameters  $\Delta H^\ddagger$ ,  $\Delta S^\ddagger$ , and  $\Delta V^\ddagger_{\text{exptl}}$  are listed in Table 3, together with the corresponding data reported for other  $\text{Co}(\text{N}_5)\text{Cl}^{2+}$  complexes.

Table 4. Rate constants  $k_{\text{OH}}$  at variable temperature and variable ionic strength<sup>[a]</sup>

$T$ [K]	$k_{\text{obsd}}/[\text{OH}^-]$ [ $\text{M}^{-1}\text{s}^{-1}$ ] ( $I = 0.1$ NaClO <sub>4</sub> ) <sup>[b]</sup>	$k_{\text{obsd}}/[\text{OH}^-]$ [ $\text{M}^{-1}\text{s}^{-1}$ ] ( $I = 1.0$ NaNO <sub>3</sub> ) <sup>[c]</sup>
288	(2.45 ± 0.01) × 10 <sup>-2</sup>	(0.905 ± 0.003) × 10 <sup>-2</sup>
293	(5.76 ± 0.08) × 10 <sup>-2</sup>	(2.35 ± 0.06) × 10 <sup>-2</sup>
298	(13.9 ± 0.1) × 10 <sup>-2</sup>	(5.34 ± 0.06) × 10 <sup>-2</sup>
308	(75.2 ± 0.2) × 10 <sup>-2</sup>	(26.4 ± 0.1) × 10 <sup>-2</sup>
318	(335.7 ± 0.3) × 10 <sup>-2</sup>	(124.3 ± 0.5) × 10 <sup>-2</sup>

<sup>[a]</sup>  $[\text{CoLCl}^{2+}] = 2.5 \cdot 10^{-3}$  M. — <sup>[b]</sup>  $[\text{OH}^-] = 0.025$  M. — <sup>[c]</sup>  $[\text{OH}^-] = 0.065$  M.

The  $\Delta H^\ddagger$  and  $\Delta S^\ddagger$  values obtained for **2** are conspicuously close to those of the “parent complex”  $\text{Co}(\text{NH}_3)_5\text{Cl}^{2+}$ , which undergoes base hydrolysis at a similarly low rate.<sup>[25]</sup> The large positive entropy of activation of ca. 150  $\text{Jmol}^{-1}\text{K}^{-1}$  has often been discussed as a mechanistic proof for the equilibrium according to Equation 8a.<sup>[26]</sup> The value of  $\Delta V^\ddagger_{\text{exptl}} = 27.6 \pm 0.6 \text{ cm}^3 \text{mol}^{-1}$  (cf. Experimental Section) provides strong evidence that base hydrolysis of complex **2** follows the  $\text{D}_{\text{cb}}$  mechanism. By way of comparison, the average base hydrolysis volume of activation of 11 different dipositive (amine)cobalt(III) complexes is 29.7  $\text{cm}^3 \text{mol}^{-1}$ ,<sup>[24]</sup> and thus close to the value found in the present study. In the same way as  $k_{\text{OH}} \equiv kK$ ,  $\Delta V^\ddagger_{\text{exptl}}$  is a composite parameter, involving the contri-

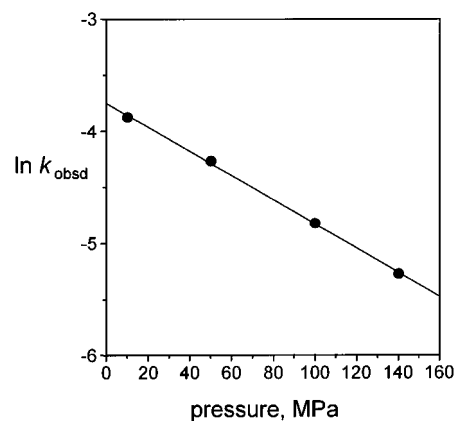


Figure 5. Plot of  $\ln k_{\text{obsd}}$  vs. pressure for base hydrolysis of complex **2** according to Equation 12 at 308 K ( $[\text{complex}] = 2.5 \cdot 10^{-3}$  M;  $[\text{OH}^-] = 0.1$  M;  $I = 1.0$  M NaNO<sub>3</sub>)

bution of the pressure dependence of the equilibrium of Equation 8a,  $\Delta \bar{V}(K)$ , and that of the rate-determining dissociation step of Equation 8b,  $\Delta V^\ddagger(k)$ , according to Equation 11. For  $\text{Co}^{\text{III}}$  complexes with an overall 2+ charge, the magnitude of  $\Delta \bar{V}(K)$  can be estimated<sup>[24,27]</sup> to be  $+19.3 \pm 1.5 \text{ cm}^3 \text{mol}^{-1}$ , resulting in an activation volume  $\Delta V^\ddagger(k)$  of  $8.3 \text{ cm}^3 \text{mol}^{-1}$  for the reaction step of Equation 8b.

$$\Delta V^\ddagger_{\text{exptl}} = \Delta \bar{V}(K) + \Delta V^\ddagger(k) \quad (11)$$

This value is smaller when compared to  $\Delta V^\ddagger(k) = 14.5 \text{ cm}^3 \text{mol}^{-1}$  for the complex  $\text{Co}(\text{NH}_3)_5\text{Cl}^{2+}$ ,<sup>[28a]</sup> but within the experimental error limits not small enough to indicate convincingly an  $\text{I}_d$ -controlled reaction of the deprotonated intermediate  $\text{CoL-HCl}^+$  (see Equation 8b) as opposed to a  $\text{D}$ -controlled one.<sup>[28b]</sup> The overall  $\Delta V^\ddagger_{\text{exptl}}$  value therefore favors the operation of a  $\text{D}_{\text{cb}}$  mechanism. The difference in  $\Delta V^\ddagger(k)$  found for **2** and  $\text{Co}(\text{NH}_3)_5\text{Cl}^{2+}$  probably reflects the rigidity of the tetrapodal ligand L, which makes the

formation of a five-coordinate intermediate very unfavorable and hinders the dissociation of the intermediate amide complex according to Equation 8b.

### Conclusions Concerning the D<sub>cb</sub> Mechanism

There has been a lot of controversy as to whether deprotonation in the step of Equation 8a, leading to the conjugate base, occurs at the most acidic amino proton. <sup>1</sup>H-NMR studies provided strong evidence that this is not necessarily so.<sup>[12,23]</sup> It was therefore repeatedly concluded that the differences in the rate of base hydrolysis are mainly governed by the lability of the conjugate base rather than by differences in proton labilities of the parent complex. Questions of this sort need not to be considered for **2**, where the *trans* position is occupied by a 2,6-disubstituted pyridine. Deprotonation can thus occur only at one of the four equivalent amino groups *cis* to the leaving chloride ion.

It is well established that the lability of the amido conjugate base depends significantly on the constraints imposed by the geometry and structure of the ligand(s):

- 1) A meridional or “flat” secondary nitrogen atom (such as the central nitrogen atom in the ligand dien), *cis* to the leaving group, leads to high base hydrolysis rates. In the case of facial coordination (resulting in a “bent” secondary nitrogen atom), hydrolysis occurs at a notably lower rate.<sup>[21]</sup>
- 2) Five-membered chelate rings on either side of a “flat” nitrogen atom favor rapid hydrolysis, especially in the presence of additional six-membered chelate rings.<sup>[21]</sup>
- 3) A pyridine ligand *cis* to the leaving group increases the rate of base hydrolysis markedly.<sup>[10,11]</sup>
- 4) The geometry and structure of the chelating ligand determine how readily the complex will form a five-coordinate amide intermediate of trigonal bipyramidal geometry, which is considered to be the most favorable geometry.<sup>[12,21]</sup>

When the first two of these conditions are fulfilled, base hydrolysis can indeed be extraordinarily fast, as in the case of the complex cation Co(tmd)(dien)Cl<sup>2+</sup>, which has a secondary “flat” nitrogen atom *cis* to the chloride ligand as well as five-membered chelate rings on either side ( $k_{\text{OH}} = 5 \cdot 10^5 \text{ M}^{-1}\text{s}^{-1}$ ; see Table 3). When the ligand dien in this complex is coordinated facially, with the secondary “bent” nitrogen atom *trans* to chloride, the reaction rate constant is reduced to  $k_{\text{OH}} = 10.6 \text{ M}^{-1}\text{s}^{-1}$ .

According to the four requirements mentioned above, base hydrolysis of complex **2** is expected to be slow, because (i) there are no secondary NH protons at all, (ii) the pyridine ligand is not *cis* to the leaving group, and (iii) the rigid ligand L does not favor the formation of an intermediate of trigonal bipyramidal geometry.

It is interesting to note that base hydrolysis of the complex *t*-Co(tren)(NH<sub>3</sub>)Cl<sup>2+</sup> is also especially slow ( $k_{\text{OH}} = 0.02 \text{ M}^{-1}\text{s}^{-1}$ ; see Table 3). The ligand tren in this complex is a tripodal ligand of the type N(NH<sub>2</sub>)<sub>3</sub> with its tertiary nitrogen donor coordinated *trans* to chloride, whereas in **2**

the ligand L is tetrapodal and of the type N(NH<sub>2</sub>)<sub>4</sub>. One may argue, therefore, that it is the tripod or tetrapod structural element that causes reduced flexibility and, as a consequence, low base hydrolysis rates. The comparison of the complexes Co(NH<sub>3</sub>)<sub>5</sub>Cl<sup>2+</sup> and **2** shows, however, that this argument is of limited value. Both complexes show similarly low base hydrolysis rates and have virtually the same values of  $\Delta H^\ddagger$  and  $\Delta S^\ddagger$  (see Table 3), while the difference in ligand flexibility could not possibly be greater. Compared to **2**, Co(NH<sub>3</sub>)<sub>5</sub>Cl<sup>2+</sup> should easily form the trigonal bipyramidal amide conjugate base. Still, base hydrolysis is practically as slow as in the case of **2**. This may suggest that the rate at which cobalt(III) complexes of the type Co‘N<sub>5</sub>‘Cl<sup>2+</sup> follow the D<sub>cb</sub> mechanism will also be affected by the symmetry of the species Co‘N<sub>5</sub>‘Cl<sup>2+</sup>. In contrast to most of the other complexes listed in Table 3, both Co(NH<sub>3</sub>)<sub>5</sub>Cl<sup>2+</sup> and **2** are highly symmetrical in the ground state and deprotonation reduces this high degree of symmetry substantially.

A pseudo-base mechanism has been discussed to account for the rate enhancement which is observed when a pyridine ligand is coordinated *cis* to the leaving group, but there is little experimental evidence to substantiate this assumption.<sup>[12,29]</sup> A pyridine ligand *trans* to the leaving group is a structural element which had so far been lacking in the chemistry of Co‘N<sub>5</sub>‘Cl<sup>2+</sup> complexes, despite a number of attempted syntheses.<sup>[11,12]</sup> The present results clearly prove that a *trans*-coordinated pyridine ligand does not have any significant labilizing effect on the leaving group, and reinforce the analogy between the tetrapodal pentadentate ligand L and the classical pentaammine donor set.

### Experimental Section

AgClO<sub>4</sub> and NaClO<sub>4</sub> · H<sub>2</sub>O (Fluka; reagent grade) were used without further purification. (**CAUTION:** Perchlorate salts are potentially explosive; they should be handled with caution and in small quantities only!). [CoLCl]Cl(ClO<sub>4</sub>) · H<sub>2</sub>O was prepared as described.<sup>[2]</sup> Deionized water was doubly distilled in a quartz apparatus before use.

[CoL(OH)](ClO<sub>4</sub>)<sub>2</sub> (**4**): In non-basic aqueous solution, the removal of coordinated chloride from [CoLCl]Cl(ClO<sub>4</sub>) · H<sub>2</sub>O by addition of two equivalents of AgClO<sub>4</sub> and heating to 80 °C for 1 h was not complete. Complex **4** was therefore prepared by keeping a basic aqueous solution of [CoLCl]Cl(ClO<sub>4</sub>) · H<sub>2</sub>O (110 mg, 0.22 mmol, 10 mL 0.3 M NaOH, pH = 13–14) at 80 °C for 1 h. The solution was neutralized with HClO<sub>4</sub> (pH = 6–8), and 2 equivalents of AgClO<sub>4</sub> were added to remove chloride by precipitation of AgCl, which was separated by filtration. Addition of one equivalent of NaClO<sub>4</sub> · H<sub>2</sub>O to the filtrate induced crystallization. Within a few days, **4** separated from solution in the form of orange-red crystals, suitable for X-ray structure analysis (88 mg, 76% yield). – <sup>1</sup>H NMR ([D<sub>6</sub>]DMSO, r.t.):  $\delta$  = 8.21 [t, <sup>3</sup>J(HH) = 7.9 Hz, 1 H, H<sup>4</sup>], 7.73 [d, <sup>3</sup>J(HH) = 7.9 Hz, 2 H, H<sup>3,5</sup>], 4.70 (m, br., NHH), 4.52 (m, br., NHH), 2.67 (m, CHHNH<sub>2</sub>, 4 H), 2.26 (m, CHHNH<sub>2</sub>, 4 H), 1.47 (s, 6 H, CH<sub>3</sub>), –2.60 [s (br.), *W*<sub>1/2</sub> = 7.1 Hz, OH]. – <sup>13</sup>C NMR ([D<sub>6</sub>]DMSO, r.t.):  $\delta$  = 165.32 (s, C2/6), 140.46 (s, C4), 120.48 (s, C3/5), 46.51 (s, >C<), 44.83 (m, 3 lines, *J* = 7.8 Hz, CH<sub>2</sub>), 21.17 (s, CH<sub>3</sub>). – MS (FAB<sup>+</sup>); *m/z* (relative intensity): 409 (48) [M – OH + ClO<sub>4</sub>], 79 (100), C<sub>5</sub>H<sub>5</sub>N. – MS (ESI<sup>+</sup>): 326 (100) [M – H], 308 (76) [M – H<sub>2</sub>O – H], correct isotope patterns in both cases.

– IR (KBr):  $\tilde{\nu}$  = 3578 cm<sup>-1</sup> (m), 3294 (s), 2972 (m), 1610 (m), 1471 (m), 1093 (vs), 624 (m). – C<sub>13</sub>H<sub>26</sub>Cl<sub>2</sub>CoN<sub>5</sub>O<sub>9</sub> (526.22): calcd. C 29.67, H 4.98, N 13.31; found C 29.42, H 4.95, N 13.18.

**Instrumentation:** UV/Vis spectra, diode array spectrophotometer (Zeiss Specord S10); NMR spectra, FT-NMR spectrometer (JEOL JNM-EX 270); mass spectra, Micromass ZabSpecE spectrometer; IR spectra, FT-IR spectrometer (Nicolet, Impact 400); pH measurements, glass electrode (Schott) in combination with a potentiometer (Metrohm 691), calibrated at  $I = 0.1$  M (NaNO<sub>3</sub>) and 25°C to yield  $-\log[H^+] = \text{pH} - 0.09$ ; kinetics of base hydrolysis, multi-wavelength stopped-flow spectrophotometer<sup>[30]</sup> and stopped-flow spectrophotometer in combination with a high-pressure cell.<sup>[31]</sup>

**Spectrophotometric Titration:** The acid dissociation constant  $K_a$  of **3** according to Equation 4 was determined by spectrophotometric titration of an acid solution of **3** with 0.1 M NaOH. Least-squares fitting of Equation 5 to the (absorbance,  $[H^+]$ ) data led to  $K_a$  ( $A_{H_2O}$  and  $A_{OH}$  refer to the absorbance of **3** and **4**, respectively, at the concentration of  $[Co]_{tot}$ ).

**Kinetic Measurements:** Base hydrolysis of **2** according to Equation 3 in freshly prepared solutions of  $[CoLCl]Cl(ClO_4) \cdot H_2O$  in water was followed by stopped-flow spectrophotometry in the wavelength range 300–600 nm under pseudo-first-order conditions ( $[OH^-] \gg [complex]_0$ ) at variable temperature (285–318 K) and variable pressure (10–150 MPa). The reactions were followed for  $t = 6$ –8 half-lives. Monitoring at high pressure was done at 480 nm. The ionic strength was set to  $I = 0.1$  M or 1.0 M (NaClO<sub>4</sub> or NaNO<sub>3</sub>). Least-squares fitting of the (absorbance, time) data with Equation 6 led to the experimental rate constant  $k_{obsd}$ . The volume of activation was obtained from the pressure dependence of  $k_{obsd}$  according to Equation 12. A correction for the pressure dependence of the activity coefficients (less than 0.6 cm<sup>3</sup> mol<sup>-1</sup> under the given conditions<sup>[32]</sup>) was not applied.

$$\Delta V^\ddagger_{exptl} = -RT (\partial \ln k_{obsd} / \partial P)_T \quad (12)$$

**Crystallography:** The crystal of **3** (orange-red platelet, 0.45 × 0.40 × 0.17 mm) was grown as stated above. The measurement was made with a four-circle diffractometer (Stoe-Stadi-4) using graphite-monochromatized Mo- $K_\alpha$  radiation ( $\lambda = 0.71069$  Å); scan  $2\theta/\omega = 1:1$ . Cell constants were determined by the least-squares method from the  $2\theta$  angles of 50 reflections. The structure was solved by direct methods with SHELXS-86 and refined by least squares to the  $R$  values given in Table 5 using the program package SHELXL-93. The non-hydrogen atoms were refined anisotropically. All hydrogen atoms, including that in the hydroxo ligand, were located in the difference Fourier map. The hydrogen atom positions and a uniform isotropic displacement parameter were kept fixed during refinement. An empirical absorption correction was applied ( $T_{min} = 0.693/T_{max} = 0.799$ ). The residual electron density was +0.624/−0.409 e Å<sup>-3</sup>. Crystal data and data collection parameters are listed in Table 5, and selected distances and angles are given in Table 2. Crystallographic data (excluding structure factors) for the structure reported in this paper have been deposited with the Cambridge Crystallographic Data Centre as supplementary publication no. CCDC-103018. Copies of the data can be obtained free of charge on application to CCDC, 12 Union Road, Cambridge CB2 1EZ, UK [Fax: int. code + 44-1223/336-033; E-mail: deposit@ccdc.cam.ac.uk].

Table 5. Crystallographic data for  $[CoL(OH)](ClO_4)_2$  (**4**)

Empirical formula Formula mass		C <sub>13</sub> H <sub>26</sub> Cl <sub>2</sub> CoN <sub>5</sub> O <sub>9</sub> 526.22	
$a$	16.841(6) Å	space group	$C2/m$ (no. 12)
$b$	8.541(3) Å	$T$	299(2) K
$c$	15.112(5) Å	$\lambda$	0.71069 Å
$\beta$	109.13(1)°	$\mu$	1.153 mm <sup>-1</sup>
$V$	2053.7(12) Å <sup>3</sup>	$R I^{[a]}$ [ $I > 2\sigma(I)$ ]	0.0352
$Z$	4	$wR2^{[b]}$	0.1070
$D_{calcd.}$	1.702 g cm <sup>3</sup>		

<sup>[a]</sup>  $RI = \sum |F_o| - |F_c| / \sum |F_o|$ . – <sup>[b]</sup>  $wR2 = \{\sum [w(F_o^2 - F_c^2)^2] / \sum [w(F_o^2)^2]\}^{1/2}$ , where  $w = 1/[\sigma^2(F_o^2) + 0.0627 P^2 + 1.845 P]$  and  $P = (F_o^2 + 2 F_c^2)/3$ .

## Acknowledgments

Sponsorship of this work by the Deutsche Forschungsgemeinschaft, the Verband der Chemischen Industrie and the Otto-Röhm-Stiftung is gratefully acknowledged. The authors appreciate the co-operation with Stefan Schmidt (preparation of the chloro complex), Carlos Dücker-Benfer (high-pressure stopped-flow experiments), Frank W. Heinemann (refinement of the X-ray data) and W. Donaubauer (measurement of the mass spectra).

- [1] C.-H. Lee, B. Garcia, T. C. Bruice, *J. Am. Chem. Soc.* **1990**, *112*, 6434.
- [2] A. Grohmann, F. Knoch, *Inorg. Chem.* **1996**, *35*, 7932.
- [3] M. E. de Vries, R. M. La Crois, G. Roelfes, H. Kooijman, A. L. Spek, R. Hage, B. L. Feringa, *J. Chem. Soc., Chem. Commun.* **1997**, 1549.
- [4] C. Dietz, S. Schmidt, F. W. Heinemann, A. Grohmann in *Selective Reactions of Metal-Activated Molecules* (Eds.: H. Werner, P. Schreier), Vieweg, Braunschweig, **1998**, p. 217.
- [5] C. Dietz, F. W. Heinemann, J. Kuhnigk, C. Krüger, M. Gerdan, A. X. Trautwein, A. Grohmann, *Eur. J. Inorg. Chem.* **1998**, 1041.
- [6] A. Grohmann, F. W. Heinemann, P. Kofod, *Inorg. Chim. Acta*, in press.
- [7] For an elegant recent study of (cyclen)cobalt(III) complexes, see: D. A. Buckingham, C. R. Clark, A. J. Rogers, J. Simpson, *Inorg. Chem.* **1998**, *37*, 3497.
- [8] M. L. Tobe, *Adv. Inorg. Bioinorg. Mech.* **1983**, *2*, 1.
- [9] An authoritative, brief summary of the arguments leading to the establishment of the conjugate base mechanism may be found in: R. G. Wilkins, *Kinetics and Mechanism of Reactions of Transition Metal Complexes*, VCH, Weinheim, **1991**, p. 215.
- [10] J. McKenzie, D. A. House, *J. Inorg. Nucl. Chem.* **1977**, *39*, 1843.
- [11] B. R. Cameron, D. A. House, A. McAuley, *J. Chem. Soc., Dalton Trans.* **1993**, 1019.
- [12] E. Ahmed, C. Chatterjee, C. J. Cooksey, M. L. Tobe, G. Williams, M. Humanes, *J. Chem. Soc., Dalton Trans.* **1989**, 645.
- [13] J. Burgess, *Metal Ions in Solution*, Wiley, Chichester, **1978**, p. 271.
- [14] [14a] A. Looney, R. Han, K. McNeill, G. Parkin, *J. Am. Chem. Soc.* **1993**, *115*, 4690. – [14b] R. Alsasser, M. Ruf, S. Trofimenko, H. Vahrenkamp, *Chem. Ber.* **1993**, *126*, 703.
- [15] H.-O. Kalinowski, S. Berger, S. Braun, <sup>13</sup>C-NMR-Spektroskopie, Thieme, Stuttgart, **1984**, p. 512.
- [16] G. Socrates, *Infrared Characteristic Group Frequencies*, Wiley, Chichester, **1994**, p. 223.
- [17] A recent search of the Cambridge Crystallographic Data Base for terminal Co<sup>III</sup>–OH complexes produced 2 hits:
- [17a] A. Bigotto, E. Zangrando, L. Randaccio, *J. Chem. Soc. Dalton Trans.* **1976**, 96. – [17b] E. S. Kucharski, B. W. Skelton, A. H.

- White, *Aust. J. Chem.* **1978**, *31*, 47.
- [18] J. D. Atwood, *Inorganic and Organometallic Reaction Mechanisms*, VCH, New York, **1996**, p. 48.
- [19] A. Bondi, *J. Phys. Chem.* **1964**, *68*, 441.
- [20] The kinetic data shown in Figure 4 are based on experiments in which  $I = 0.1$  M was adjusted with  $\text{NaClO}_4$  and  $I = 1.0$  M with  $\text{NaNO}_3$ , due to limited solubility of the cobalt complex in 1 M  $\text{NaClO}_4$ . It was shown, however, that there is no spectrophotometrically detectable interaction between 1 M  $\text{NaNO}_3$ , and  $\text{CoCl}^{2+}$  and  $\text{CoLOH}^{2+}$  respectively.
- [21] R. Henderson, M. L. Tobe, *Inorg. Chem.* **1977**, *16*, 2576.
- [22] W. G. Jackson, B. C. McGregor, S. S. Jurrison, *Inorg. Chem.* **1990**, *29*, 4677.
- [23] P. Comba, W. G. Jackson, W. Marty, L. Zipper, *Helv. Chim. Acta* **1992**, *75*, 1147.
- [24] Y. Kitamura, G. A. Lawrance, R. van Eldik, *Inorg. Chem.* **1989**, *28*, 333.
- [25] L. S. Dong, D. A. House, *Inorg. Chim. Acta* **1976**, *19*, 23.
- [26] J. O. Edwards, F. Monacelli, G. Ortaggi, *Inorg. Chim. Acta* **1974**, *11*, 47.
- [27] Y. Kitamura, R. van Eldik, *Ber. Bunsenges. Chem.* **1984**, *88*, 418.
- [28] [28a] Y. Kitamura, R. van Eldik, H. Kelm, *Inorg. Chem.* **1984**, *23*, 2038. — [28b] A. Drljaca, C. D. Hubbard, R. van Eldik, T. Asano, M. V. Basilevsky, W. J. le Noble, *Chem. Rev.* **1998**, *98*, 2167.
- [29] D. A. House, P. R. Norman, R. W. Hay, *Inorg. Chim. Acta* **1980**, *45*, L117.
- [30] H. Elias, F. Sattler, K. J. Wannowius, *GIT Fachz. Lab.* **1985**, *29*, 1138.
- [31] R. van Eldik, W. Gaede, S. Wieland, J. Kraft, M. Spitzer, D. A. Palmer, *Rev. Sci. Instrum.* **1993**, *64*, 1355.
- [32] R. van Eldik, Y. Kitamura, C. P. Piriz Mac-Coll, *Inorg. Chem.* **1986**, *25*, 4252.
- [33] R. G. Pearson, R. E. Meeker, F. Basolo, *J. Am. Chem. Soc.* **1956**, *78*, 709.
- [34] D. A. Buckingham, P. J. Cresswell, A. M. Sargeson, *Inorg. Chem.* **1975**, *14*, 1485.

Received September 18, 1998  
[I98316]